Dielectrophoretic Segregation of Different Human Cell Types on Microscope Slides

ARTICLE *in* ANALYTICAL CHEMISTRY · JUNE 2005

Impact Factor: 5.64 · DOI: 10.1021/ac048196z · Source: PubMed

6 AUTHORS, INCLUDING:

Chandra M Das
University of Texas MD Anderson Cancer Center
5 PUBLICATIONS **153** CITATIONS
SEE PROFILE

Suzanne D Vernon
103 PUBLICATIONS **3,354** CITATIONS
SEE PROFILE

Peter R C Gascoyne
Advanced Electrofluidic Systems, LLC
118 PUBLICATIONS **6,002** CITATIONS
SEE PROFILE

Anal. Chem. **2005,** *77,* 2708−2719

Dielectrophoretic Segregation of Different Human Cell Types on Microscope Slides

Chandra M. Das,† Frederick Becker,† Suzanne Vernon,‡ Jamileh Noshari,† Celine Joyce,† and Peter R. C. Gascoyne*,†

Department of Molecular Pathology, The University of Texas M. D. Anderson Cancer Center, 1515 Holcombe Boulevard, Houston, Texas 77030, and Centers for Disease Control and Prevention, 1600 Clifton Road MSA15, Atlanta, Georgia 30333

A new method for preparing cells for microscopic examination is presented in which cell mixtures are fractionated by dielectrophoretic forces and simultaneously collected into characteristic zones on slides. The method traps cells directly from the suspending medium onto the slide, reducing cell loss. Furthermore, it exploits differences in the dielectric properties of the cells, which sensitively reflect their morphology. Because different cell types are trapped in characteristic zones on the slide, the technique represents an advance over existing methods for slide preparation, such as centrifugation and smears where cells are randomly distributed. In particular, the new method should aid in the detection of rare and anomalous cell subpopulations that might otherwise go unnoticed against a high background of normal cells. As well as being suitable for traditional microscopic examination and automated slide scanning approaches, it is compatible with histochemical and immunochemical techniques, as well as emerging molecular and proteomic methods. This paper describes the rationale and design of this so-called electrosmear instrumentation and shows experimental results that verify the theory and applicability of the method with model cell lines and normal peripheral blood subpopulations.

Advances in cytological slide preparation techniques have facilitated the identification and characterization of different cell types and have improved the ease and accuracy of disease diagnosis. In particular, numerous staining procedures, including chemical dye-,[1] fluorescent-,[2] and enzyme-linked,[3] immunosensitive,[4] and specific molecular methods[5] have been developed. While these techniques allow target cells to be differentiated from other cell types, specimen screening efficiency depends on how well the pathologist discriminates target components such as bacteria, precancerous lesions, or cancerous cells from background cells. In diseases characterized by the presence of extremely small numbers of marker cells against a background of large numbers of normal cells, identifying the randomly distributed target cells is tedious, time consuming, and prone to error. Recently, a number of instruments have been introduced that automatically scan slides and attempt to identify putative marker cells for later review by a pathologist.[6] These instruments are based on machine vision through a high-quality microscope, and they are expensive and relatively slow.

One approach to improving the rapidity and accuracy of screening by both manual and automated methods would be the generation of smears in which each cell subtype is segregated into a characteristic spatial zone. In this way, the location of specific cell types on a slide would be known in advance of screening and the examination process could be greatly accelerated. A method capable of localizing cells by type is dielectrophoresis (DEP), a technique that has been used to separate cancer cells from blood[7] and from CD34+ hematopoetic stem cells,[8] bacteria from blood,[9] and the cell subpopulations of blood.[10] Distinct from electrophoresis, DEP is the movement of cells in a nonuniform electric field arising from the interaction between the field and field-induced charge polarization on the cells[11] and does not depend on the net charge of the cells. Because cell dielectric properties depend sensitively on their morphology,[12−14] cells of different types and in different physiological states experience

* Corresponding author. Telephone: (713)-792-4534. Fax: (713)-792-5940. E-mail: peter@dielectrophoresis.org.

† The University of Texas M. D. Anderson Cancer Center.

‡ Centers for Disease Control and Prevention.

(1) Lyon, H. O.; De Leenheer, A. P.; Horobin, R. W.; Lambert; W. E.; Schulte, E. K.; Van Liedekerke, B.; Wittekind, D. H. *Histochem. J.* **1994**, *26* (7), 533−44.

(2) Espada, J.; Horobin, R. W.; Stockert, J. C. *Histochem. Cell Biol.* **1997**, *108* (6), 481−7.

(3) Bennett, R. W. In *Bacteriological Analytical Manual*, 8th ed., Revision A; Food and Drug Administration, AOAC Int.: Gaithersburg, MD, 1998; Chapter 13A.

(4) Retallack, R. In *Immunocytochemical analysis of sperm cytoskeleton. Tested studies for laboratory teaching*; Goldman, C. A., Ed.; OmniPress: Madison, WI, 1995; Vol. 16, pp 135−40.

(5) Horobin, R. W.; Rashid, F. *Histochemistry* **1990**, *94* (2), 205−9.

(6) Zbigniew, D.; Elzbieta, B.; Xun, Li, Wojciech G.; Myron, R. *Exp. Cell Res.* **1999**, *249* (1), 1−12.

(7) Gascoyne, P. R. C.; Wang, X.-B.; Huang, Y.; Becker, F. F. *IEEE Trans. Ind. Appl.* **1997**, *33* (3), 670−8.

(8) Huang, Y.; Yang, J.; Wang, X.-B.; Becker, F. F.; Gascoyne, P. R. C. *J. Hematother. Stem Cell Res.* **1999**, *8*, 481−90.

(9) Markx, G. H.; Huang, Y.; Zhou, X.-F.; Pethig, R. *Microbiology* **1994**, *140*, 585−91.

(10) Yang, J.; Huang, Y.; Wang, X.-B.; Becker, F. F.; Gascoyne, P. R. C. *Biophys. J.* **2000**, *78*, 2680−9.

(11) Pohl, H. A. *Dielectrophoresis*; Cambridge University Press: Cambridge, U.K., 1978.

(12) Huang, Y.; Wang, X.-B.; Becker, F. F.; Gascoyne, P. R. C. *Biochim. Biophys. Acta* **1996**, *1282*, 76−84.

(13) Fuhr, G.; Hagedorn, R. *Electrical Manipulation of cells*; Chapman and Hall: New York, 1996; pp 37−66.

(14) Pethig, R.; Kell, D. B. *Phys. Med. Biol.* **1987**, *32*, 933−70.

10.1021/ac048196z CCC: $30.25
Published on Web 03/24/2005

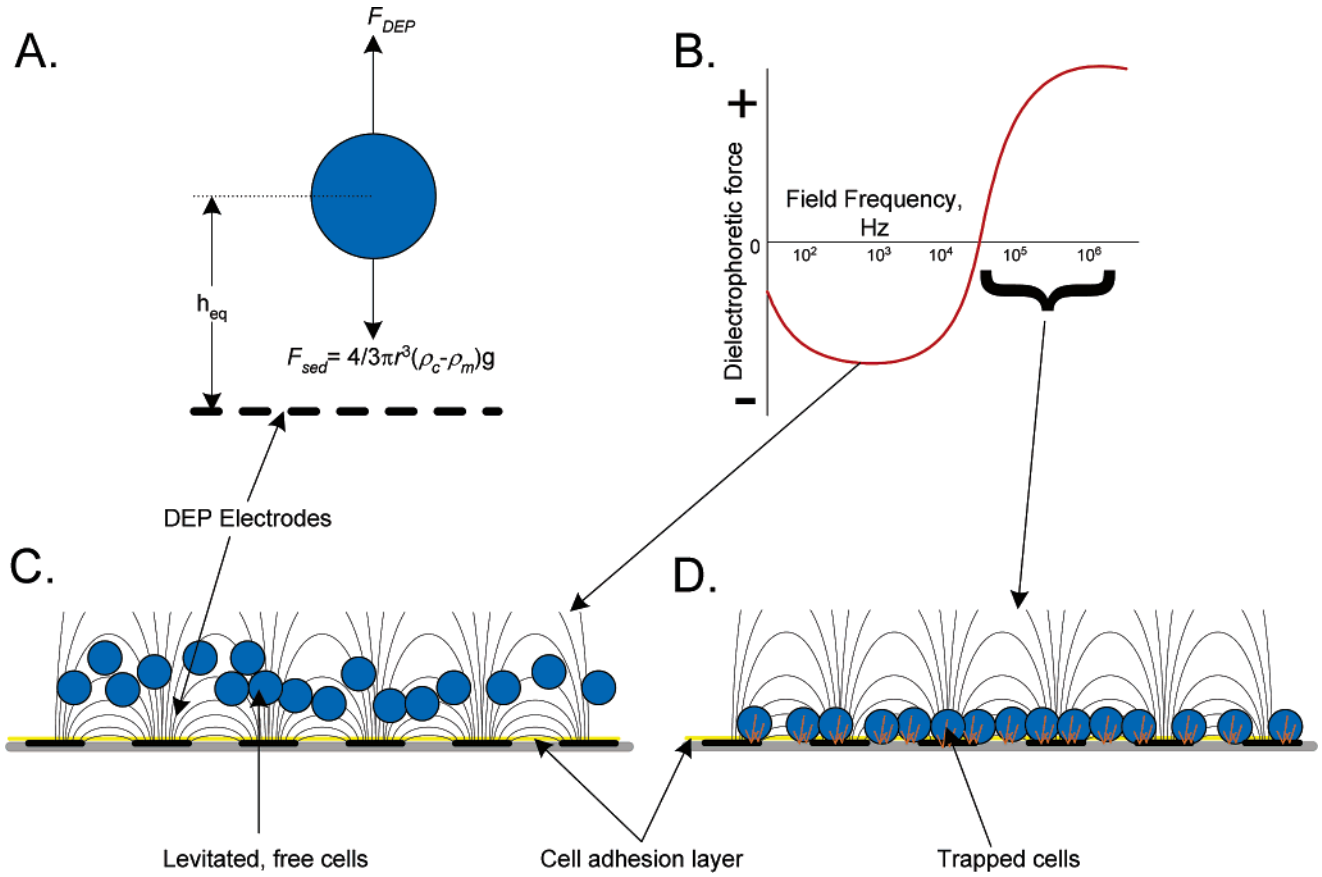

Figure 1. (A) Cells levitated above an electrode array by repulsive DEP forces. Because the DEP forces decrease with increasing height above the electrode, a cell will reach an equilibrium height h_{eq} where the DEP forces are balanced by the sedimentation forces of gravity. (B) The DEP force acting on a cell depends on the frequency of the applied electrical field. At low frequencies, the DEP force is repulsive. At some higher frequency, a cell characteristic called the crossover frequency, the DEP force will fall to zero, and at still higher frequencies, the DEP force will attract the cell to the electrodes. (C) The electrosmear slide has an array of DEP electrodes and is coated with a cell adhesion layer (such as polylysine). For electric fields below the crossover frequency, DEP forces levitate cells above the adherent surface of the slide, preventing them from sticking, and cells can travel freely above the slide surface. (D) Fore electric fields at and above the crossover frequency, the DEP forces do not levitate the cells, which touch down onto the adherent surface and become trapped for subsequent analysis.

different DEP forces, allowing them to be spatially discriminated[15–17] in appropriate ac electric field distributions.

In this article, we describe a method that uses a microscope slide coated with a cell binding agent and patterned with a thin electrode array that is excited with electrical signals to provide DEP forces on cells. Cells are introduced at one end of the slide where DEP forces provide a levitation force that opposes cell sedimentation and prevents them from adhering to the binding agent. The excitation signal applied to the electrodes, and hence the levitation characteristics, vary along the slide. Cells flow along the slide above the binding agent until they reach a region in which the DEP forces resulting from the spatially variant excitation signals are no longer sufficient to levitate them. At that position they "touch down" and adhere to the binding agent. Using this approach, heterogeneous cell suspensions may be processed to produce segmented smears in which the constituent cell subpopulations collect in different, characteristic zones. This method is suitable for the preparation of slides for microscopic examination by pathologists and automated slide readers, as well as other analytical methods that benefit from having different cell types spatially isolated—such as SELDI and MALDI-TOF. In this report, we explain the basis of the methodology, show two practical implementations, and illustrate the technique with examples of blood cells, cancer cells, and cultured cell lines.

THEORY

The principle of the electrosmear method can be understood from the force diagram in Figure 1A, where cells are shown levitated above an adhesive surface of a microscope slide by a DEP force. The DEP force acting on a cell in the vertical direction above a set of parallel electrodes can be approximated as

$$F_{\mathrm{DEP}} = 2\pi\epsilon_{\mathrm{m}}(r/d)^3\hat{f}_{\mathrm{CM}}AV^2\mathrm{e}^{-h/2\pi d} \qquad (1)$$

where V is the rms value of the applied ac voltage, h is the height of the cell above the electrode plane, d is the periodicity of the parallel electrode elements, A is a constant pertaining to the electrode geometry ($A = 2.76$ for a planar parallel electrode array), and ϵ_{m} is the electrical permittivity of the buffer in which the cells

(15) Gascoyne, P. R. C.; Huang, Y.; Pethig, R.; Vykoukal, J.; Becker, F. F. *Meas. Sci. Technol.* **1992**, *3*, 439−45.
(16) Markx, G. H.; Pethig, R. *Biotechnol. Bioeng.* **1995**, *45*, 337−43.
(17) Wang, X.-B.; Huang, Y.; Gascoyne, P. R. C.; Becker, F. F.; Holzel, R.; Pethig, R. *Biochim. Biophys. Acta* **1994**, *1234*, 185−94.

are suspended.[18,19] This equation assumes that the cells experience dipolar forces and that higher order terms do not significantly affect cell levitation. It represents the average force seen by cells as they travel through the electric field profile, which actually varies with cell position with respect to electrode edges and gaps. Although, in principle, DEP forces arise from either dc or alternating fields, eq 1 assumes that electrode polarization has a negligible impact on the field seen by the cells. This is typically satisfied for ac fields above ~20 kHz in frequency. The parameter $\hat{f}_{CM}$ is the *real* part of the so-called Clausius−Mossotti factor, a dielectric parameter that reflects the properties of the cells and the characteristics of their suspending medium.[20−22] This may be written as

$$\hat{f}_{CM} = \left(\frac{f^2 - f_0^2}{f^2 + 2f_0^2}\right) \tag{2}$$

where f is the frequency of the applied electric field and f_0 is the so-called crossover frequency at which the DEP force changes from being repulsive to attractive with increasing frequency for a particular cell type[12,23,24] (see Figure 1B). When $f < f_0$, $\hat{f}_{CM}$ is negative, resulting in a repulsive DEP force that can levitate the cell above the electrode plane and away from the adhesive surface of the slide. For a viable cell type having an intact plasma membrane, f_0 can be approximated as

$$f_0 = \sigma_s/2^{(1/2)}\pi r C_{mem} = \Theta\sigma_s \tag{3}$$

where σ_s is the conductivity of suspending medium, r is the radius of the cell, and C_{mem} is the cell-specific plasma membrane capacitance.[7,12,25] Equation 3 assumes that the cell plasma membrane barrier function is intact so that transmembrane conductivity is small compared with that of the suspending medium. The expression demonstrates that each cell type having a different characteristic combination of radius and plasma membrane capacitance has a unique crossover frequency that can be defined by a parameter Θ. Morphologically distinct cell types have different dielectric phenotypes,[7,26] allowing DEP to be utilized for cell discrimination and manipulation. This is especially useful in applications such as cytology where morphological characteristics are critical determinants of cell identity and correspond to different physiologic and pathologic states. Equation 3 also shows that in general cellular DEP responses scale with the conductivity of the suspending buffer, allowing significant control of the desired effects. We have provided elsewhere more general expressions than eq 3 for leaky cells in which membrane electrical conduction effects contribute to the DEP properties and for cells having nonspherical morphology while in suspension.[24]

In addition to the DEP force, the cells in Figure 1A experience a sedimentation force given by

$$F_{sed} = (4/3)\pi r^3(\rho_p - \rho_m)g \tag{4}$$

where g is the acceleration due to gravity and ρ_p and ρ_m are the densities of the cell and suspending buffer, respectively. Combining eqs 1 and 4, we find that a repulsive DEP force and the sedimentation force will balance when the height of the cell above the electrode plane is given by[10,19,27]

$$h_{eq} = 2\pi d \log\left(\frac{-3\epsilon_m \hat{f}_{CM} A V^2}{2(\rho_p - \rho_m)g d^3}\right) \tag{5}$$

(see Figure 1C). The condition for a cell to touch down on the electrode plane occurs as $h_{eq} \rightarrow 0$ (see Figure 1D). Using eq 2, this condition may be written conveniently in terms of the cell characteristics as

$$\frac{-V^2}{(\rho_p - \rho_m)}\left(\frac{f^2 - f_0^2}{f^2 + 2f_0^2}\right) = \frac{2gd^3}{3\epsilon_m A} \tag{6}$$

where the cell properties are embodied in $\rho_p - \rho_m$ (the difference in density between the cell and its suspending buffer) and the cell crossover frequency f_0 given by eq 3.

Equation 6 is the basic equation of the electrosmear technique. By providing a distribution along the length of a slide of the applied electric field conditions, cells having characteristic density and f_0 combinations may be induced to settle at different distances along the slide corresponding to the conditions where $h_{eq} \rightarrow 0$ for each cell type. Two special cases of the electrosmear can be envisaged, one in which the DEP frequencies are varied along the length of the slide while the applied peak-to-peak voltage is held constant, and the other in which the DEP frequencies are held constant along the length of the slide while the peak-to-peak voltage is varied.

To realize the first of these embodiments, a series of sets of interdigitated electrodes spaced along a slide were energized with different frequency signals, beginning with the lowest frequency signal where cells entered at one end of the slide and with subsequent sets energized with increasingly higher frequencies as shown diagrammatically in Figure 2A. This approach was mechanically complex to give enough different frequency zones to provide good cell discrimination, requiring (in our embodiment) one connection to each of 36 electrode sets along the length of the slide and a signal generator network that simultaneously provided 36 different frequencies.

The second embodiment, employing spatially varying voltages rather than frequencies, was mechanically simpler because it could

(18) Wang, X.-B.; Yang, J.; Vykoukal, J.; Becker, F. F.; Gascoyne, P. R. C. *Anal. Chem.* **2000**, *72* (4), 832−9.
(19) Huang, Y.; Wang, X.-B.;, Becker, F. F.; Gascoyne, P. R. C. *Biophys. J.* **1997**, *73*, 1118−29.
(20) Jones, T. B. *Electromechanics of Particles*; Cambridge University Press: Cambridge, U.K.. 1995; Chapter 3, pp 34−80.
(21) Sauer, F. A. *Interaction between Electromagnetic Fields and Cells*; Plenum Publishing Corp.: New York, 1985; pp 181−202.
(22) Wang, X.-B.; Huang, Y.; Gascoyne, P. R. C.; Becker, F. F. *IEEE Trans. Ind. Appl.* **1997**, *33* (3), 660−9.
(23) Chan, K. L.; Gascoyne, P. R. C.; Becker, F. F.; Pethig, R. *Biochim. Biophys. Acta* **1997**, *1349*, 182−96.
(24) Gascoyne, P. R. C.; Pethig, R.; Satayavivad, J.; Becker, F. F.; Ruchirawat, M. *Biochim. Biophys. Acta* **1997**, *1323*, 240−52.
(25) Yang, J.; Huang, Y.; Wang, X.; Wang, X.-B.; Becker, F. F.; Gascoyne, P. R. C. *Biophys. J.* **1999**, *76*, 3307−14.
(26) Gascoyne, P. R. C. *Tumor markers−Physiology, Pathobiology, Technology, and Clinical Applications*; AACC Press: New York, 2002; Chapter 53.
(27) Wang, X.-B.;, Vykoukal, J.; Becker, F. F.; Gascoyne, P. R. C. *Biophys. J.* **1998**, *74*, 2689−701.

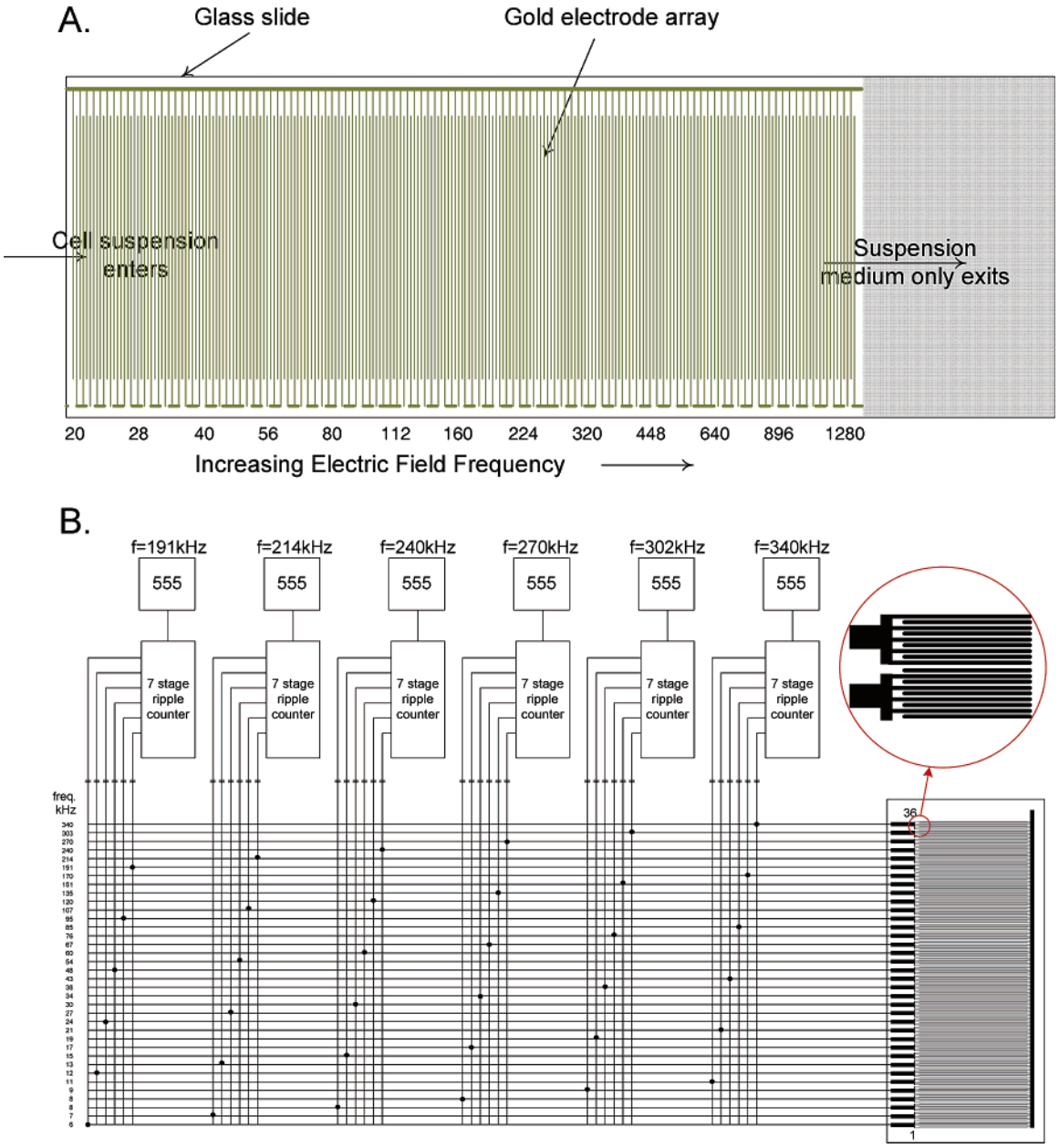

Figure 2. (A) Concept of the electrosmear in which the applied electric field frequency is controlled spatially, increasing from left (where cell suspension enters) to right (where suspension devoid of cells exits) along the slide. (B) Multifrequency signal generator used in realizing the spatial-frequency dependence. The circuit provides 36 different frequencies to excite separate groups of electrodes (shown in circle) each of which comprised 10 individual electrode elements.

be realized with a single set of interdigitated electrodes along the length of the slide and two thin bus lines connected at either end (for a total of four connections). Different ac waveforms were applied to each bus line, one to provide a repulsive DEP force and the other an attractive force. The peak-to-peak voltage of the signals was varied along the length of each bus line by exploiting the electrical resistance of each bus.

In addition to its mechanical simplicity, this approach also afforded the advantage of being programmable because it was possible to use direct digital synthesis (DDS) chips to provide complex DEP excitation waveforms to each of the buses to allow the discrimination of the electrosmear to be altered electronically. To understand the basis for this capability, we note that the time-averaged DEP force on a cell resulting from *two* simultaneously applied ac fields of different frequencies is, by superposition theory,

$$F_{\mathrm{DEP}} = 2\pi\epsilon_{\mathrm{m}}A(r/d)^3(\hat{f}_{\mathrm{CM1}}V_1^2 + \hat{f}_{\mathrm{CM2}}V_2^2)\mathrm{e}^{-h/2\pi d} \quad (7)$$

If V_1 consists of a rapidly swept frequency, then the net DEP force is

$$F_{\mathrm{DEP}} = 2\pi\epsilon_{\mathrm{m}}A(r/d)^3(\langle\hat{f}_{\mathrm{CM1}}\rangle V_1^2 + \hat{f}_{\mathrm{CM2}}V_2^2)\mathrm{e}^{-h/2\pi d} \quad (8)$$

where $\langle\hat{f}_{\mathrm{CM1}}\rangle$ is the value of the Clausius−Mossotti factor for the cell averaged over the frequency range of the rapidly swept field. For a field that is linearly and repeatedly swept between

frequencies f_1 and f_2, we can write

$$\langle \hat{f}_{CM1} \rangle = \frac{1}{(f_2 - f_1)} \int_{f_1}^{f_2} \left(\frac{f^2 - f_0^2}{f^2 + 2f_0^2} \right) \partial f \qquad (9)$$

Or, for a field logarithmically and repeatedly swept between those frequencies,

$$\langle \hat{f}_{CM1} \rangle = \frac{1}{\log(f_2/f_1)} \int_{f_1}^{f_2} \left(\frac{f^2 - f_0^2}{f^2 + 2f_0^2} \right) \partial \log(f) \qquad (10)$$

Note that cell types having different crossover frequencies will exhibit different values of $\langle \hat{f}_{CM1} \rangle$ in such swept frequency fields, and by appropriately choosing f_1 and f_2, the values of $\langle \hat{f}_{CM1} \rangle$ may be made to be different, yet positive, for all cell types. The key to being able to program the discrimination of the electrosmear using such a swept field is that the relative differences between $\langle \hat{f}_{CM1} \rangle$ values for different cell types may be altered by adjusting f_1 and f_2.

To exploit these properties in an electrosmear, a field of fixed frequency that provides negative DEP to all cell types may be applied to one side of the interdigitated electrode array. The bus line that carries this fixed frequency excitation to the interdigitated elements is configured as a metal film resistor, and the amplitude of the applied signal, V_2, is made greater at the end of the slide where cells enter than it is at the other end. The swept frequency signal is applied to the opposite bus line, also configured as a metal film resistor, and is excited by a field amplitude, V_1, having an amplitude that is smaller at the end of the slide where cells enter than it is at the other end. This excitation scheme is shown in Figure 3A. The amplitude of the fixed frequency field decreases with distance along the slide from the cell inlet while the amplitude of the swept frequency field increases. Consequently, the negative DEP force that levitates cells decreases with increasing distance from the inlet while the positive DEP force that promotes attraction to the electrodes increases with distance. Using the same arguments regarding the competition between levitation and sedimentation used for the first electrosmear embodiment having multiple segments, cells having different dielectric properties will touch down and adhere to the slide surface when

$$\frac{\langle \hat{f}_{CM1} \rangle V_1(x)^2 + \hat{f}_{CM2} V_2(x)^2}{(\rho_p - \rho_m)} = \frac{2gd^3}{3\epsilon_m A} \qquad (11)$$

Because the voltages $V_1(x)$ and $V_2(x)$ explicitly depend on the distance x from the cell inlet, different cell types will adhere in characteristic zones depending on their dielectric properties embodied in $\langle \hat{f}_{CM1} \rangle$ and their differential density $\rho_p - \rho_m$. Figure 3B shows a simulation based on eqs 9 and 11 that reveals the expected attachment location for idealized cells on an electrosmear slide as a function of cell crossover frequencies for three different settings of the excitation signals. In the steepest curve, the entire length of the electrosmear slide may be used to investigate cells having crossover frequencies between 45 and ~90 kHz. In the shallowest curve, the entire length of the electrosmear slide spans crossover frequencies from 40 to ~185 kHz. This simulation demonstrates that the discrimination of the electrosmear between different cell types can be adjusted electrically.

As indicated, in addition to being easily programmed for discrimination, the second electrosmear method, although theoretically more complex, is simpler to realize practically and offers several advantages over the multisegment electrode embodiment since only four connections are needed for the electrodes and only two frequency sources, based on programmable DDS chips, are required.

EXPERIMENTAL SECTION

Sample Preparation. Seven tumor cell lines were used in this study to validate the electrosmear method. MDA-231, MDA-435, and MDA-468 cell lines were originally obtained from pleural effusion of human breast cancer patients at the University of Texas, M. D. Anderson Cancer Center by Cailleau et al.[28] These lines have been shown to have different abilities to form tumors and to metastasize in nude mice. They were cultured and maintained in MEM media supplemented with 10% fetal bovine serum (Atlanta Biologicals, Norcross, GA), 1 mM L-glutamine, 1% penicillin, and streptomycin solution (Sigma, St. Louis, MO) as described previously.[7]

The human leukemia cell line HL-60 was originally obtained from ATCC (Manassas, VA) and was cultured as described earlier.[19] All of these cell lines have been used previously in our laboratory, and their dielectric properties are fully characterized.[7,19,29]

SW-756, a human cervical cancer line, was obtained from the department of Gynecological Oncology at U.T.M.D. Anderson Cancer Center and was cultured in MEM media containing Earl salts, 1% nonessential amino acids, 1% L-glutamine, 1% penicillin and streptomycin, and 10% fetal bovine serum. Jurkat and SK1 cell lines were gifts from Dr. Frederic Gilles at M.D. Anderson Cancer Center. Jurkat (a human T-cell leukemia cell line) and SK1 (a lymphoma cell line derived from a patient with relapsed, diffuse large cell lymphoma that expresses a highly glycosylated product of the MUC1 gene[30]) were cultured in RPMI 1640 media supplemented with 10% and 20% fetal bovine serum, respectively.

Cells were harvested from complete media by centrifugation at 1500 rpm for 10 min, and they were resuspended at a density of (1−20) × 10^6 cells/mL in isotonic 8.5% sucrose (w/w) and 0.3% dextrose (w/w) buffer. The conductivity of the final suspension was adjusted with RPMI to target values from 10 to 56 mS/m with the aid of a conductometer (Cole-Parmer Instrument, Chicago, IL). The viability of cells was always greater than 90% as determined by trypan blue dye exclusion.

Buffy coats containing mostly leukocytes were obtained from fresh peripheral blood (5−10 mL) donated by healthy volunteers at U.T.M.D. Anderson Cancer Center. Blood was collected into EDTA Vacutainers and centrifuged at 1500 rpm for 10 min in Seditubes (Becton Dickinson, Franklin Lakes, NJ). The upper layers containing leukocytes from each Seditube were mixed, washed, and suspended in the isotonic 8.5% sucrose (w/w) and 0.3% dextrose (w/w) buffer at a concentration of (50−100) × 10^6

(28) Cailleau, R.; Olive, M.; Cruciger, Q. V. *J. In Vitro* **1978**, *24*, 911−5.
(29) Becker, F. F.; Wang, X.-B.: Huang, Y.: Pethig, R.; Vykoukal, J. *Proc. Natl. Acad. Sci. U.S.A.* **1995**, *92*, 860−4.
(30) Gilles, F.; Goy, A.; Remache, Y.; Shue, P.; Zelenetz, A. D. *Blood* **2000**, *95*, 2930−6.

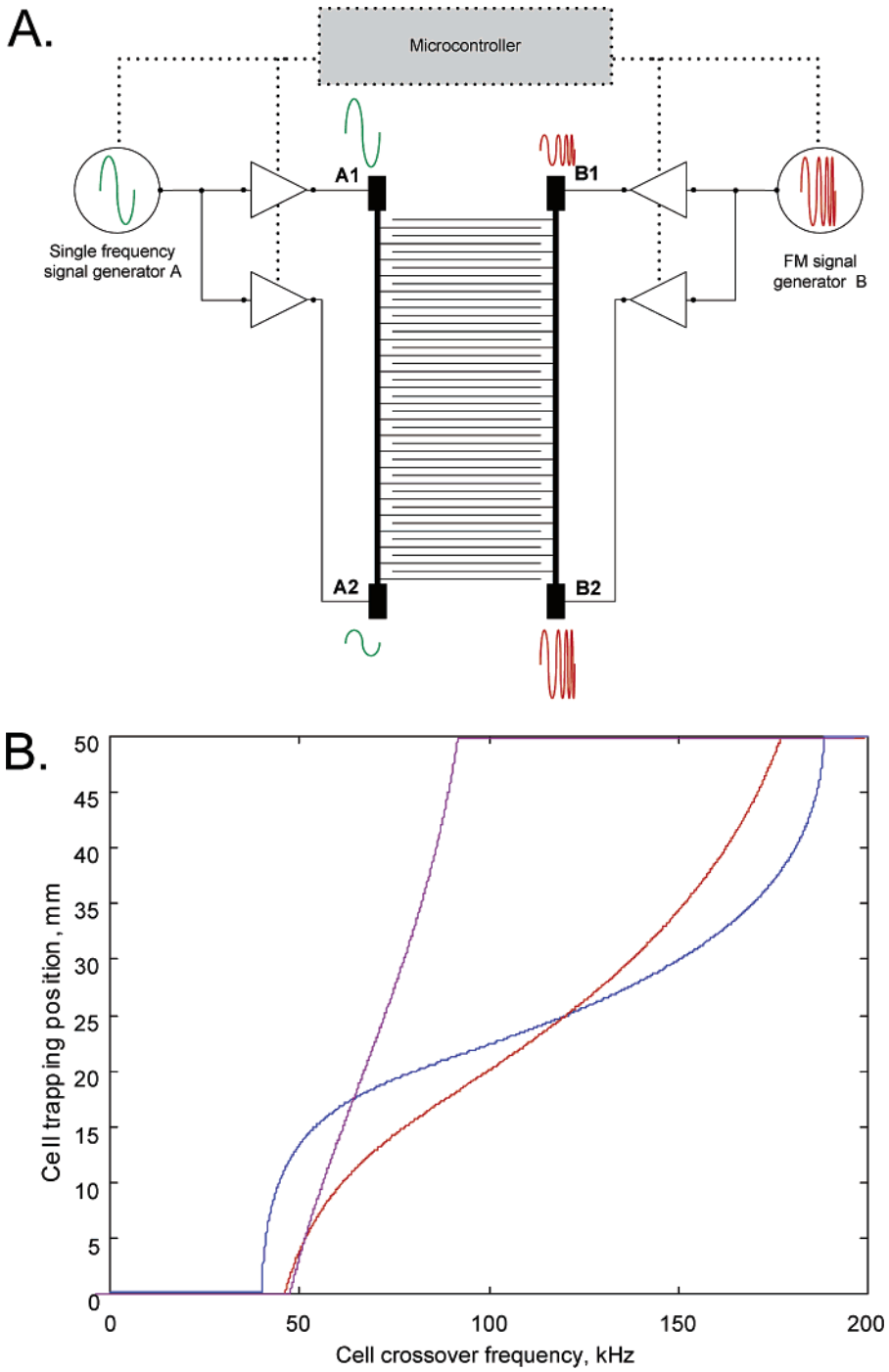

Figure 3. (A) Electrosmear method in which the frequencies were held constant and field intensities were varied spatially. Two DDS chips provided waveforms for the two bus lines, each end of which were driven by signals of different intensity. The DEP force experience by the cells resulted from the sum of the fields. The drive amplifiers were configured so that the fixed frequency signal (which provided a net negative DEP force on all cell types) was strongest at the cell inlet end (near A1 and B1) and weakest at the exit (near A2 and B2). Conversely, the swept frequency signal (which provided a net positive, though different, DEP force on all cell types) was weakest at the cell inlet end and strongest at the exit. When appropriately configured, the net DEP force acting on all cells was negative at the inlet and fell to zero at different characteristic distances along the slide for different cell types. (B) Simulations, based on eq 11, show the position in millimeters along the electrosmear slide at which cells of different crossover frequencies would be trapped for three different settings of the swept frequency and drive voltages. Settings for the simulations were as follows: (i) swept frequency 10−200 kHz; 1 V at inlet end, 3 V at outlet end; (ii) swept frequency 10−398 kHz; 1 V at inlet end, 3 V at outlet end; (iii) swept frequency 10−398 kHz; 0 V at inlet end, 3 V at outlet end. In all simulations, the fixed frequency was 40 kHz, 3 V at the inlet end and 1.5 V at the outlet end. These simulations show that the cell trapping discrimination can be programmed over a wide range by this method.

cells/mL. The cell suspensions were adjusted to target conductivities between 10 and 56 mS/m as required. Buffy coats derived by this method were contaminated by erythrocytes as judged from the color of the cell pellets. These were also examined in the electrosmear process. Viability of blood cells was greater than 95% by trypan blue dye exclusion.

To obtain monocyte-enriched preparations, we used the RosetteSep cocktail purchased from Stem Cell Technologies (Vancouver, BC, Canada) according to the protocol provided with the product.

In short, blood was incubated with 50 μL of cocktail/mL of blood for 20 min. The sample was diluted with an equal volume of PBS containing 2% FBS and 1 mM EDTA and layered on top of Ficoll−Paque followed by centrifugation at 2400 rpm for 20 min at room temperature with the brake off. Monocyte-enriched cells were collected from the Ficoll−Paque plasma interface.

In some experiments, catalase (C40, Sigma Chemical) was added to the sucrose/dextrose buffer at a concentration between 24 and 1200 ng/mL to investigate possible cell damage effects due to hydrogen peroxide generated electrochemically during electrical field exposure on the electrosmear slides.[31]

Electrosmear Chamber. Electrodes were custom manufactured by Thin Film Technology (Buellton, CA) by microphotolithographically patterning 0.3-μm gold over 50-nm titanium on a glass substrate. In experiments using spatially dependent frequencies, slides were patterned with 36 groups each comprising 10 gold electrodes of 50-μm width and 50-μm spacing (see Figure 2B). Each electrode group was energized by a different frequency from a custom-built signal generator via gold finger contacts along one side of the slide. The interdigitated counter electrodes were connected to a single bus line running the length of the other side of the slide. A custom-built signal generator applied frequencies to the electrode groups that increased in a geometric progression (six steps per octave) either from 6 to 384 kHz or from 20 kHz to 1.28 MHz in different experiments. The peak-to-peak excitation voltage for each frequency was held constant at 3.3 V.

For the spatially dependent voltage approach, the 36 groups of electrodes were shorted to an additional bus line at the very edge of the slide to form a single bank of interdigitated electrodes that covered the entire length of the slide. By controlling the width of the bus lines and the metalization thickness, the resistance of each bus line from one end to the other was set to approximately 5−10 Ω, allowing each bus to be used as a potential divider to control the voltages applied to the electrodes distributed along its length. A custom signal generator employing two DDS channels generated separate fixed and swept frequency signals for the two respective buses. Each DDS channel was equipped with two variable gain power amplifier outputs that could be adjusted from 0 to 5 V peak-to-peak to drive different signal levels into each end of the bus lines (see Figure 3A). Bus voltages were typically 0.5 V peak-to-peak at one end and 3.5 V peak-to-peak at the other, and the potential divider characteristics of each resistive bus line resulted in spatial distributions of the signal intensities along the slide. The fixed frequency signal was typically 20 kHz, and the swept signal was typically a linear sweep from 20 to 800 kHz repeated 200 times/s. Instantaneous adjustment of the discrimination and trapping characteristics of this embodiment of the electrosmear was made possible by programmable, and instantly implementable, alterations of the DDS signals and power amplifier output gains via a microcontroller embedded in the signal generator. Whereas the spatially dependent frequency approach required 40 connections to the electrosmear slide, the variable voltage approach required only 4 contacts. This allowed the variable voltage arrangement to have much larger and more reliable contact areas and a greatly simplified holder than the variable frequency arrangement.

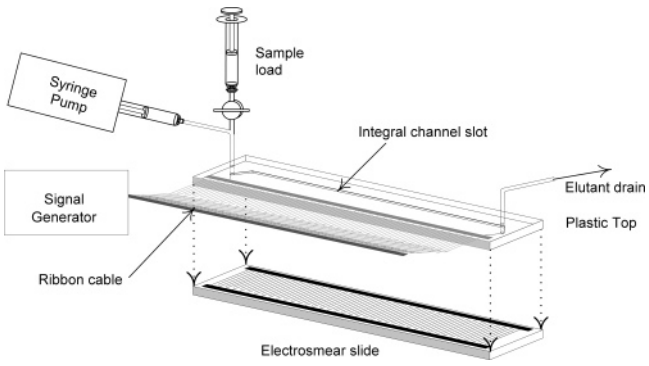

Figure 4. Exploded view of the electrosmear assembly. The specimen loading mechanism shown is for a high concentration of cells delivered from a syringe. For dilute cell suspensions, the sample can be loaded directly from the syringe pump and the cells trapped directly from the specimen suspension medium as it passes through the electrosmear chamber. Note the mechanical simplicity of the design to ensure that cells are not lost during slide preparation.

To prepare the cell-adherent surfaces, slides were cleaned in Piranha solution (concentrated H_2SO_4/H_2O_2 in a 7:3 ratio) for 2 min, rinsed with triple distilled H_2O, dried in an N_2 stream, and then coated with polylysine solution (p8920, Sigma) for 2 h. Finally, the slides were rinsed, dried again in an N_2 stream, and used for electrosmear experiments. The polylysine treatment has been shown to ensure that cells adhere once they touched the surface of the slides.

The assembly used to hold the electrosmear slides during cell trapping is shown in Figure 4. The separation chamber was formed by sandwiching a slotted Teflon spacer between a plastic top plate and the electrosmear slide on the bottom. The chamber dimensions were 45 mm long, 10 mm wide, and 400 μm high. Flow of eluant through ports at either end of the chamber was controlled at rates of 50−100 μL/min by a digital syringe pump (Daigger, Wheeling, IL).

Separation. The electrosmear chamber was first filled with degassed 8.5% sucrose and 0.3% dextrose eluant buffer at different conductivities between 10 and 56 mS/m. An aliquot of 20 μL of cell sample suspended in the same buffer was introduced into the chamber through the injection port, and a brief flow of eluant into the inlet end of the chamber from the digital syringe pump was used to transport the cells into the entrance of the chamber. The pump was then turned off, and the cells were allowed to sediment (to "relax") for 5 min to reach equilibrium heights according to their dielectric properties (see eq 5). Cells were assured of being levitated above the adhesive coating of the slide by the repulsive DEP forces at the inlet end of the chamber. After relaxation of the cells, eluant flow from the digital syringe pump was initiated with the same buffer to transport the cells through the separation chamber and, thereby, along the electrosmear slide.

As each cell type reached the region where the repulsive DEP forces no longer overcame sedimentation, those cells settled and adhered to the polylysine coating of the slide. In this way, each cell type adhered in a different characteristic zone. The fluid flow

(31) Wang, X.; Yang, J.; Gascoyne, P. R. C. *Biochim. Biophys. Acta* **1999**, *1426*, 53−68.

rate used to transport the cells was chosen to ensure that they adhered to the surface, and that they were not dragged along, after they touched down in their characteristic zones. This was satisfied at flow rates up to 100 mL/min using the polylysine-adherent coating employed here. It is possible that alternative coatings could be used to bind cells more effectively than polylysine and thereby allow faster flow rates to be used.

Staining. After each run, slides were removed from the chamber and air-dried. To facilitate the identification of cell types, the electrosmear slides were fixed and stained with a Hema Diff (Stat Lab Medical Productive, Lewisville, TX) staining kit used according to the manufacturer's instructions. Finally, the slides were mounted with coverslips, observed under the microscope, and photographed.

RESULTS

Electrosmears of Cultured Cell Lines. Three cultured tumor cell lines, SW-756 (cervical), SKI (B cell lymphoma), and Jurkat (T cell leukemia) were trapped in different characteristic locations on electrosmear slides. For experiments using the electrosmear embodiment having segmented electrode sets and spatially dependent frequencies and at a suspension medium conductivity of 50 mS/m, SW-756 was trapped in a single band between 75 and 85 kHz, and SK1 was trapped between 74 and 149 kHz. Interestingly, Jurkat cells were trapped in four distinct bands between 114 and 192 kHz. An electrosmear slide revealing this discrete banding pattern of Jurkat cells is illustrated in Figure 5, which shows that subpopulations of cells were trapped on different groups of electrodes energized by different DEP frequencies. That this banding pattern reveals heterogeneity in the Jurkat line, as opposed to an artifact in electrosmear function, is indicated by the fact that some cells were captured as soon as they experienced the DEP forces above an excitation zone and landed predominantly at the leading edge of that zone. Other cells having slightly higher crossover frequencies remained levitated until they became trapped at the leading edge of an electrode group of higher frequency. The heterogeneity in the Jurkut cell line was consistent and was verified through several independent runs using similar growth conditions. It was not associated with cell aggregation.

Typical trapping zone results for three breast cancer lines, MDA-231, MDA-435 and MDA-468, and the human myelogenous leukemia HL-60 cell line as a function of suspension medium conductivity are shown in Figure 6. The three breast cancer lines were trapped at frequencies of 13−15, 17−27, and 48−74 kHz at conductivities of 10, 20, and 50 mS/m, respectively. Trapping frequencies for HL60 were significantly different compared with the breast cancer lines especially at higher conductivities. At a conductivity of 10 mS/m, HL-60 was trapped at frequencies 15−17 kHz (close to the breast cancer lines), but at higher conductivities, HL-60 was trapped at much higher frequencies (28−74 kHz at 20 mS/m and 74−149 kHz at 50 mS/m). The trapping frequencies for both breast cancer lines and HL-60 increased with increasing conductivity in a linear fashion, but at different rates with different intercepts. The rate of increase of crossover frequency of HL-60 was roughly double that of the breast cancer lines.

Electrosmear Characterizations of Mixed Cell Populations. Blood Cell Subpopulations. Buffy coat preparations from several normal healthy individuals were subjected to electrosmear

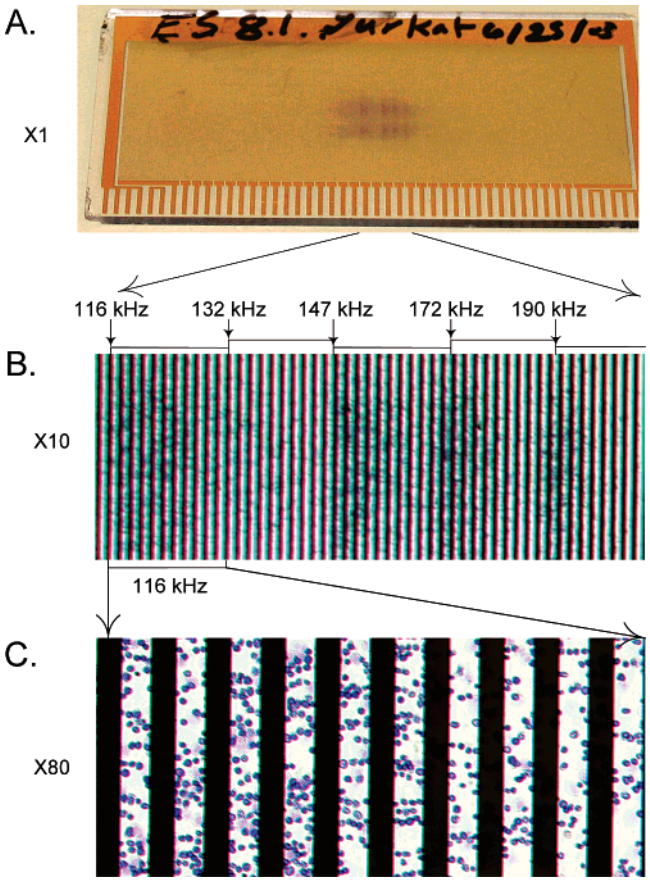

Figure 5. Electrosmear result for Jurkat cells revealing banding pattern and heterogeneity in the cells. (A) Photograph of the electrosmear slide, showing the gold contacts that were energized by different frequency signals and the trapping distribution of the cells. (B) A 10× magnification of the trapping zones for the Jurkat cells, revealing that cells having slightly different DEP properties were trapped on different groups of electrodes corresponding to different DEP excitation frequencies. (C) An 80× magnigication of the subpopulation of Jurkat cells that were trapped in the 114-kHz region of the electrosmear slide.

analysis at conductivities of 10, 20, and 50 mS/m, and the results are shown in Figure 7. Three main bands corresponding to mixed granulocytes, lymphocytes, and erythrocytes adhered in three different zones at all conductivities. In the lowest frequency zone, granulocytes predominated mixed with a lesser number of lymphocytes. The middle frequency zone contained pure lymphocytes, and the highest frequency zone contained pure erythrocytes. This pattern of trapping was similar for all conductivities, but the trapping zone for each cell type was shifted to higher frequencies with increasing buffer conductivity in a linear fashion. For example, erythrocytes were trapped between 56 and 76, 85 and 96, and 298 and 356 kHz at conductivities of 10, 20, and 50 mS/m, respectively. The *relative* position of the adhesion zones for granulocytes, lymphocytes, and erythrocytes did not change significantly with increasing conductivity, though the separation of the three zones was slightly better at 50 mS/m than at the lower conductivities.

We did not observe monocytes among other leukocytes in our limited number of buffy coat preparations. This might have been due to a low abundance of monocytes in our samples or some other unidentified factor. To gather data on this important

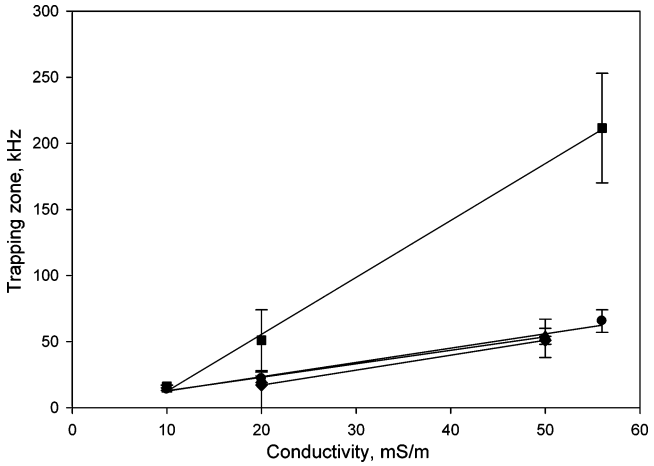

Figure 6. Dependency of the electrosmear trapping zone positions (midpoint of bands) on the conductivity of the suspending medium used as the eluant. Results shown are for (●) MDA-435, (▲) MDA-231, (◆) MDA-468, and (■) HL-60. The linear dependency of the trapping frequency with suspending medium conductivity agrees with the expectations of the eq 3.

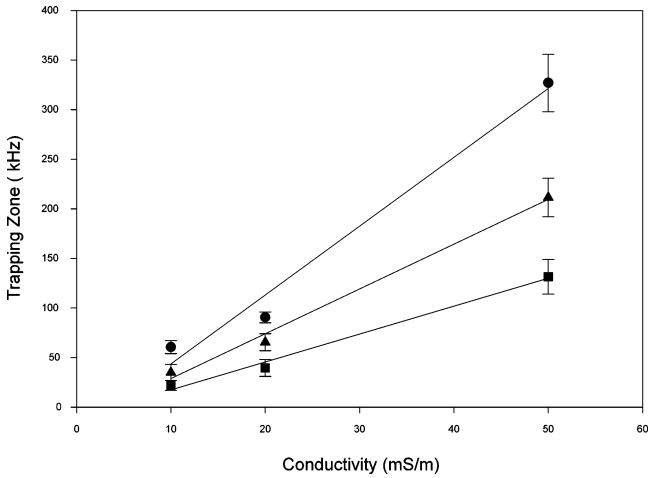

Figure 7. Dependency of the electrosmear trapping zone positions on the conductivity of the suspending medium for peripheral blood cell subpopulations: (●) erythrocytes; (▲) lymphocytes; (■) granulocytes. The linear dependency of the trapping frequency with suspending medium conductivity agrees with the expectations of the eq 3.

subpopulation, cells enriched with monocytes were prepared and processed. At a conductivity of 50 mS/m, electrosmear analysis yielded a pure population of monocytes between 149 and 171 kHz followed by a band of damaged monocytes with a few granulocytes between 192 and 216 kHz (data not shown).

Tumor Cells and Blood Cell Subpopulations. When MDA-435 (breast tumor) was mixed with a buffy coat preparation in 1:1 ratio at a conductivity of 50 mS/m and subjected to electrosmear analysis, the MDA-435 cells were trapped in a zone at 57−74 kHz followed by granulocytes 115−149 kHz, lymphocytes 192−231 kHz, and pure erythrocytes 298−345 kHz. The results of this experiment are illustrated in Figure 8. Similarly, HL-60 was separated from blood cell subpopulations when a mixture of HL-60 and buffy coat (1:1 ratio) was subjected to electrosmear analysis. Bands of HL-60 were followed by the bands of granulocytes, lymphocytes, and erythrocytes, respectively. Results are shown in Table 1. Heterogeneity in HL-60 was also revealed by a

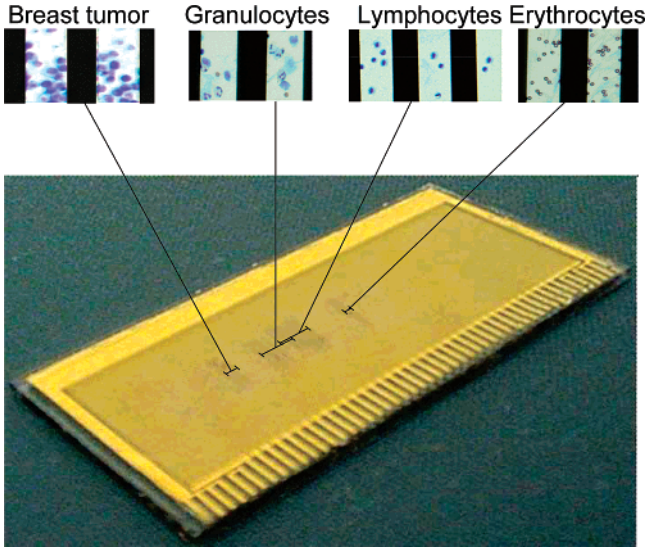

Figure 8. Photograph of an electrosmear slide revealing the banding patterns for a population of MDA-435 breast cancer cells mixed with a buffy coat from human peripheral blood. As indicated, the breast cancer cells were trapped at lowest frequency (closest to the inlet end for the sample) followed, at higher frequencies, by granulocytes, mixed granulocytes, and lymphocytes, and a pure population of erythrocytes.

band of giant cells of HL-60 followed by a band of small cells of HL-60 spanning the region between 74 and 149 kHz.

Mixed Tumor Cells. MDA-435 (breast tumor) and HL-60 (promyelocytic leukemia) cells were mixed together and subjected to electrosmear analysis. The two tumor lines settled at the same respective trapping zones as if they were processed separately. Indeed, the two lines were clearly separated from each other on the microscope slide with the band of MDA-435 cells spatially separated from the band of HL-60 cells (Table 1).

DISCUSSION

Cell levitation brought about by opposing dielectrophoretic and sedimentation forces has been used in the past as the basis for the cell separation method called hyperlayer dielectrophoretic field-flow fractionation (hyperlayer DEP-FFF) that we have described in detail elsewhere.[32] In that method, cells reach equilibrium levitation heights above an electrode array and are carried through the separation channel by a hydrodynamic flow profile that causes cell types levitated to different heights to emerge from the channel outlet at different times, thereby effecting fractionation.[10,19,27] During the course of our DEP-FFF studies, the need arose for fractionated cell subpopulations to be collected for pathological examination. For rare cell subpopulations, it proved difficult to prepare cytological slides of very small numbers of cells by cytospin and other conventional cytology methods since those methods were cumbersome and the loss of cells was significant. The electrosmear method was developed to solve this problem. Unlike DEP-FFF, the excitation signals of the electrosmear are made to vary with distance along the slide and the cells are induced to settle and adhere on the electrodes. Therefore, while DEP-FFF exploits a reusable chamber to fractionate cells according to the time at which they exit the chamber, the electrosmear

(32) Gascoyne, P. R. C.; Vykoukal, J. *Electrophoresis* **2002**, *23*, 1973−83.

Table 1. Electrosmear Trapping Characteristics for Cells in Mixture

sample mixture	conductivity (mS/m)	trapping zone for each cell type (kHz)				
		HL-60	MDA-435	granulocytes	lymphocytes	erythrocytes
buffy coat + MDA-435	50		37−74	115−149	192−231	298−345
buffy coat + HL-60	50	37 (giant cells) 74−149 (small cells)		115−149	192−231	298−345
HL-60 + MDA-435	50	75−149	38−67			

uses a disposable electrode array that permanently traps cell fractions by spatial coordinate on a slide. The DEP-dependent equilibrium levitation height (eq 5) is common to both methods, making the DEP-FFF and electrosmear methods close relatives. The chief difference between the techniques from an instrumentation perspective is that the voltage and frequency signals applied to the electrodes in DEP-FFF are typically uniform along the length of the chamber, while they must be spatially controlled in the electrosmear approach and organized to capture all of the required cells. By achieving this, the electrosmear method aims to couple cell fractionation with rare cell isolation without sample loss in a single device.

Two special cases of the electrosmear principle can be envisaged, one in which the intensity of the voltage signals is held constant over the slide while the frequency of the applied ac signals is varied and the other in which the ac signals are held constant while the intensity of the voltages is varied spatially. The basic equations for the two cases are presented here, and we built systems to test the feasibility of both approaches. While the general case in which both frequencies and voltages can be spatially varied would clearly offer the most potential for adjusting the cell capture characteristics of an electrosmear device, we found that the spatially dependent voltage approach could be built far more simply than the spatially dependent frequency approach by taking advantage of the resistive properties of the thin metal bus lines that carry power along the sides of the slide to the cell levitation/trapping electrodes. Using this thin film resistor approach, a single bank of electrodes with only 4 contacts is sufficient to realize the distributed voltage case while at least 40 contacts and numerous electrode groups are needed for the frequency-distributed case.

The cell collection results obtained for the various cell types with both electrosmear approaches showed that the electrosmear method can separate different cell types into different zones in accordance with differences in cell properties. It is useful to derive characteristic parameters for each cell type so that its banding properties may be predicted under any experimental conditions. Knowing the excitation configuration for an electrosmear slide, it is a straightforward matter to determine the zone in which each cell type was trapped. In our case, we also determined the cell density properties for each cell type. We note that eq 6 allows the cell's crossover frequency to be determined. If $V^2/\Delta\rho$ is large, then cells on the frequency-distributed electrosmear will collect in zones very close to their crossover frequencies, i.e., $f \approx f_0$. Equation 3 shows that f_0 varies linearly with the buffer conductivity, σ_s, and that a frequency parameter, $\Theta = 1/(2^{(1/2)}\pi r C_{mem}$ characterizes each cell type. A plot of f against σ_s should therefore have a slope Θ, and if required, the membrane capacitance C_{mem} can be derived from Θ if the cell radius r is measured.

Table 2. Summary of Dielectric Data for the Cells Studied by the Electrosmear Method[a]

cell type	θ (MHz·m/S)	r (μm)	C_{mem} (mF/m^2)	publ C_{mem} (mF/m^2)
erythrocytes	6.94	2.8 ± 0.1	11.6 ± 2.14	11.8 ± 0.8
lymphocytes	4.72	3.5 ± 0.2	13.6 ± 1.94	11.5 ± 1.1
granulocytes	2.87	4.71 ± 0.23	16.7 ± 2.41	11.0 ± 3.2
monocytes	3.2	4.63 ± 0.36	15.24 ± 1.04	15.3 ± 4.3
HL-60	2.3	5.8 ± 0.42	16.85 ± 6.39	16.41 ± .41
MDA- 231	1.01	6.2 ± 0.58	35.61 ± 4.91	25.9 ± 3.7
MDA-435	0.975	7.7 ± 0.58	29.97 ± 7.2	23.0 ± 7.7
MDA- 468	1.13	7.2 ± 0.66	28.41 ± 1.42	27.5 ± 4.2
Jurkat	3.06	5.92 ± 0.66	12.43 ± 4.94	
SK1	2.23	6.43 ± 0.845	15.69 ± 7.97	

[a] Values of Θ were derived from the slopes of the cell responses shown in Figures 6 and 7. The specific membrane capacitance values (C_{mem}) were computed from the Θ values using eq 3. Cell radii (r) values were either measured or obtained from previous references.

We tested the predicted linear dependency of cell trapping position on suspending medium conductivity, and as shown in Figures 6 and 7, our results are in accord with the theory. From the slope of each linear plot, the specific membrane capacitance of each cell type was calculated using eq 3 and the results are summarized in Table 2. The radii of Jurkat, SK1, and SW-756 cell lines were measured directly from cell images against a stage micrometer as described previously.[12,24] Radii for the other cell types were obtained from the literature.[7,25]

One common approach used in dielectrophoresis to characterize cells is the so-called DEP crossover frequency method in which crossover frequencies are measured directly as a function of the suspending medium conductivity and the cell dielectric parameters are deduced from plots analogous to those in Figures 6 and 7.[12,24] We have previously published electrorotation and DEP crossover[25] results for several cell lines and for blood cell subpopulations, and we compared the cell dielectric parameters obtained from the electrosmear method with those published data.[7,24,25] For the record, we found that in one of our previous papers,[7] erroneous values were calculated for two cell types and we provide corrected values here in Table 2 recalculated from the original data. As shown, capacitance values obtained from the electrosmear analysis are in close agreement with the values found previously, suggesting that the electrosmear method may be useful for rapidly measuring, as well as comparing, cell dielectric parameters of cell populations. Indeed, the method may be better than the slower approaches because it allows the properties of a very large population of cells to be examined on a cell-by-cell basis. We believe that the C_{mem} values reported here for lymphocytes and granulocytes, which are slightly higher than our published values measured by electrorotation,[25] may be more accurate than the

earlier values because in electrorotation we used relatively few cells to derive the capacitance and other dielectric parameters. Here, many thousands of cells can be seen distributed on each electrosmear in an asymmetric distribution, allowing us to calculate the mean capacitance (deduced from the slope of the lines shown in Figures 6 and 7). We also examined three cell lines (Jurkat, SK1, SW-756) for which dielectric data have not been reported previously, and the properties of these cells are shown in Table 2.

Altogether we examined seven cultured tumor lines including three breast cancer lines, one cervical cancer line, and three blood cancer lines. The properties of the cultured tumor lines of epithelial origin, including breast and cervical lines, were clearly distinguishable from those of tumor lines of lymphoid origin, e.g., HL-60, Jurkat, and SK1, and both were distinct from normal blood cell subpopulations. Therefore, the cells banded into distinct zones as shown in Table 1. The average C_{mem} value of breast cancer lines was found to be 30 mF/m^2, more than twice that of blood cell subpopulations or tumor lines of blood cell origin.

Our tests clearly showed that the cell types were trapped into the same characteristic zone whether they were subjected to electrosmear analysis as pure cell suspensions or combined into complex mixtures of multiple cell types. This demonstrated that the cell types do not interfere with one another under the conditions used for this study and shows that the electrosmear technique is useful for separating cells within complex specimens. Thus, HL-60 and MDA-435 could be separated from each other and from all of the peripheral blood cell subpopulations. The heterogeneity of cultured cell lines was also apparent from electrosmear analysis. Thus, as shown in Table 1, large and smaller HL-60 cells were segregated into two distinct bands on the electrosmear. Evidently the method provides sufficient discrimination to allow the heterogeneous population within a cell culture to be fractionated (Figure 5). All of the cell types we examined revealed heterogeneity though in most cases trapping zones were less distinct than for the Jurkat cells, which showed very distinct banding. We believe that the heterogeneity reflects cell subpopulations in different stages of the cell cycle and in different cell metabolic states. For example, we have shown previously that the activation of T lymphocytes from their resting state results in significant changes in C_{mem} and cell diameter and that additional changes in these parameters accompany each phase of the cell cycle.[19] The analysis of these changes is beyond the scope of the present article, which aims to demonstrate the electrosmear technique, but they will form the focus of future work using the methods described here. By offering a novel means of discrimination, the electrosmear approach clearly provides a new window for the analysis of cell subpopulations.

Despite its success in separating several of the cell types into nonoverlapping bands, the electrosmear method does not afford the same level of discrimination as the DEP-FFF technique from which it was derived. Thus, the blood cell subpopulations were collected into characteristic zones, but these zones overlapped somewhat, because the differences in cell capacitance and density characteristics were too small for perfect separation. Nevertheless, erythrocytes, being strikingly different, were clearly banded into a widely separated and narrow collection zone.

To establish an appropriate working range for DEP voltages, we increased the voltage levels applied to the electrosmear until cells became degenerated or damaged as evidenced by morphological changes observed after staining or by alterations detected in the cell trapping positions. The most common susceptibility of cells to damage by applied electric field is plasma membrane leakage induced by excessive transmembrane voltage. Such leakage results in a breakdown of eq 3, which gives the crossover frequency for intact cells. This in turn results in a large increase in the cell crossover frequency and a correspondingly large shift in cell capture position toward the outlet end of the electrosmear slide. Previous work suggested that voltages exceeding 4 V peak-to-peak might cause damage to cells on our 50-μm electrode configuration.[31] As expected, we did see changes especially for cells of larger size (>10 μm) at 4 V peak-to-peak, and smaller cells showed changes at higher voltages. In such cases, ghost cells, bare nuclei, pycnotic cells, or blown out cells were seen in addition to preserved trapped cells. We also looked for evidence at frequencies below 20 kHz that hydrogen peroxide formed at the electrodes and damaged cells as reported previously.[31] This effect could be mitigated by the addition of catalase to the cell suspending medium.[31] For the cell trapping experiments presented here, voltages of 3.5 V peak-to-peak or less were employed, resulting in no apparent damage to the trapped cells. In addition, in most cases we maintained the minimum frequency at 20 kHz or above and the addition of catalase was not required to maintain cell viability. As expected, damaged cells were trapped at higher frequency positions than the healthy cells so the electrosmear has a built-in indicator of experimental conditions that lead to cell damage. Interestingly, we found that HL-60 cells were more prone to damage by applied voltages than the other cell types we examined. It is noteworthy that HL-60 was chosen previously[33,34] to determine the dielectric effects of toxicants and apoptosis initiators on cells because it was found to show sensitive responses. However, we do not know whether these sensitivities are correlated. The fact that electrosmear cell trapping patterns reflect cell viability and structural integrity presents the important caveat that to obtain the most distinct cell banding patterns, attention needs to be paid to the viability of the samples.

Overall, our results clearly indicate that the electrosmear approach is a potentially powerful method for concentrating and isolating cell subpopulations from suspensions of mixed cells. Furthermore, different cell types are collected into characteristic zones on the slide, potentially allowing a pathologist to quickly screen for the presence of specific cell subpopulations. Epithelially derived tumor cells were captured at the lowest DEP frequencies, blood-related tumor cells were trapped at higher frequencies, and normal blood cell subpopulations and erythrocytes adhered in still higher frequency zones. The method captures cells directly from a cell suspension without the need to transfer it to a centrifuge or other intermediate slide-making apparatus even if the suspension is extremely dilute. As such, it seems likely that the method will be applicable to slide making for numerous applications and, in particular, for collection of rare cells from specimen such as fine needle aspiration biopsies (manuscript in preparation),

(33) Wang, X.; Becker, F. F.; Gascoyne, P. R. C. *Biochim. Biophys. Acta* **2002**, *1564*, 412−20.
(34) Ratanachoo, K.: Gascoyne, P. R. C.; Ruchirawat, M. *Biochim. Biophys. Acta* **2002**, *1564*, 449−58.

lavages, urine, and other fluids. The fact that tumor cells should be trapped in a zone that is separated from zones where normal cell types trap may decrease the risk that rare tumor cells go undetected.

Finally, the distribution of cell types on the electrosmear slides reported in this paper were analyzed by two pathologists after the slides were fixed and stained by standard methods. In addition to helping to quantify the successful aspects of cell characteristic trapping, the pathologists also helped identify the threshold of conditions under which cell damage occurred at high voltages as well as other nonideal characteristic of our current electrosmear apparatus. For example, some undesirable and inconsistent puddling of cells often occurred at the inlet region of the electrosmear slide during sample loading and during the relaxation phase. For obvious reasons, we are undertaking additional studies to understand and improve the cell injection process to eliminate this nonideality. Compared to normal slides, which collect cells completely randomly, the electrosmear method met with enthusiasm from the pathologists. Last, we did not try immunostaining or other methods for revealing molecular markers in the cells. Nevertheless, there is nothing in our approach that should preclude the use of electrosmear slides with the complete range of available methodologies for cytological, molecular, and proteomic discrimination or with laser-scanning and automated slide analysis techniques.

In conclusion, our results show that the electrosmear method can be used to prepare cytological slides in which cells having different dielectric properties are localized in characteristic zones. Two special cases of the technology, differing in the manner in which spatial dielectrophoretic forces are created, were studied and both were successful. Tumor cells were collected in zones corresponding to low-frequency trapping regions of the slide. Blood cells were also separated into zones that corresponded, with increasing trapping frequency, to granulocytes, lymphocytes, and erythrocytes. The trapping characteristics of the different cell types can be rationalized in terms of a well-defined dielectric theory. Furthermore, each cell type can be characterized by a specific dielectric parameter that allows its behavior under any electrosmear preparation condition to be predicted. Different cell types within a mixture do not interfere with one another's trapping characteristics. Therefore, the zoning profiles of cell subpopulations within complex mixtures are predictable. The segregated smears on an electrosmear slide can be stained using existing and emerging methods for identifying cell types by markers. Slides made by the method are also suitable for automated slide readers. These findings suggest that the electrosmear technique may be useful as a general-purpose, stand-alone slide preparation methodology that provides sufficient discrimination to allow useful fractionation of different cell types. Furthermore, the clear differences between the epithelial tumor and blood cell types suggests that the method may be of particular value in detecting rare tumor cells against a background of blood-related cells.

ACKNOWLEDGMENT

We are grateful for support to C.M.D. from the Centers for Disease Control under IPA09663 01. This work was supported by a grant from the National Institute of Diabetes, Digestive and Kidney Diseases RO1-DK51065. We thank Tom Anderson for the design, engineering, and fabrication of the electrosmear chambers, to Younes Javadi for making the custom electronics boards, to Dr. Jody Vykoukal for help in development of the electrosmear slides, to Dr. Jon Schwartz for microscopy and photography, and to pathologist Dr. Savitri Krishnamurthy for her analysis of the electrosmear slides and her encouragement.

Received for review December 6, 2004. Accepted February 11, 2005.

AC048196Z